2022 2nd International Conference on Electronic Information Engineering and Computer Technology (EIECT) | 979-8-3503-9956-1/22/$31.00 ©2022 IEEE | DOI: 10.1109/EIECT58010.2022.00077

Can Laser Speckle Contrast Imaging be a quantitative measurement using machine learning?

Xiaoqi Hao[1,a]
[1]Faculty of Environment and Life, Beijing University of Technology, China, No. 100 Pingleyuan, Chaoyang District, Beijing, China
[a]e-mail: 1368250188@qq.com

Shuicai Wu[1,b]
[1]Faculty of Environment and Life, Beijing University of Technology, China, No. 100 Pingleyuan, Chaoyang District, Beijing, China
[b]e-mail: wushuicai@bjut.edu.cn

Lan Lin[1,c]
[1]Faculty of Environment and Life, Beijing University of Technology, China, No. 100 Pingleyuan, Chaoyang District, Beijing, China
[c]e-mail: lanlin@bjut.edu.cn

Yixiong Chen[2,d]
[2]Beijing Science and Technology Project Manager Management Corporation Ltd, Beijing, China
[d]e-mail: chenyixiong516@msn.com

Stephen P. Morgan[3,e]
[3]Optics and Photonics Research Group, University of Nottingham Nottingham, UK
[e]e-mail: steve.morgan@nottingham.ac.uk

Shen Sun[1,f*]
[1]Faculty of Environment and Life, Beijing University of Technology, China, No. 100 Pingleyuan, Chaoyang District, Beijing, China
*Corresponding author: [f]sunshen@bjut.edu.cn

***Abstract*—Laser speckle contrast blood flow imaging (LSCI) analyzes the spatial or temporal statistical characteristics of laser speckle patterns to obtain a signal proportional to blood flow. As it can achieve real time blood flow imaging at high resolution with simple instrumental setup, LSCI has been widely applied in both clinic and research. The lack of quantitative blood flow measurement is the primary limitation. Efforts have been made to optimize LSCI from the aspects of measurement accuracy and linearity such as multi-exposure laser speckle contrast imaging (MELSCI) and AI-based (artificial intelligence) LSCI. This paper reviews LSCI in terms of basic principles, system development and quantitative measurement of LSCI. The application of machine learning in LSCI is discussed in detail. By comparing the estimated perfusion results of LSCI, MELSCI and LDI (laser Doppler blood flow imaging), we propose that using machine learning to correct LSCI to MELSCI has great potential for improving measurement linearity while retaining system simplicity.**

Key words: Laser speckle contrast imaging (LSCI), blood flow imaging, machine learning, artificial intelligence (AI), microcirculation

I. Introduction

Laser speckle contrast blood flow imaging (LSCI) is well established for non-invasively obtaining images of blood flow. LSCI was firstly applied to image capillaries on the surface of the retina[1] and cerebral cortex[2]. Along with development of this technology, it has been used for in-depth exploration such as studies on the effects of oxygen saturation, the real time evaluation of mouse carotid thrombosis model and reaction of drugs on cerebral blood flow and organs[3-5].

A LSCI system has a typical setup shown in Fig. 1. A red or near infrared (NIR) laser beam is expanded to illuminate an area of the target. A CCD camera, a frame grabber and a general-purpose computer (PC) are generally utilized to capture speckle images and perform LSCI processing. The great advantage of an LSCI system is that it can produce high-resolution blood flow perfusion images in real time with simple system setup. Nowadays, LSCI is quite mature and well developed and commercialized such as Moor Instruments (UK), Perimed (Sweden) and RWD Life Science (China) etc. It is broadly applied to a range of applications such as fundamental studies of the microcirculation[6-10]; burn depth assessment[11-12]; skin cancer studies[13-14]; wound healing[15-17]; ophthalmology[1, 18-19], cardiac activity analysis[20-21] and studies of stimulant reactions of cortical activity[2, 22-25].

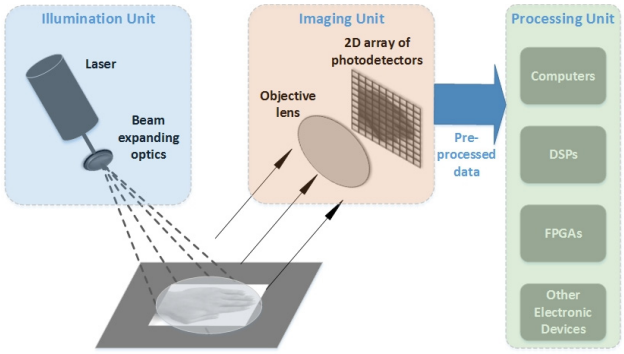

Fig. 1 Typical LSCI system setup including illumination unit, imaging unit and processing unit. Illumination unit provides divergent red/near-infrared irradiation to the target. The imaging unit captures the speckle image and transmits it to the processing unit in where the LSCI process is performed.

This paper reviews LSCI in terms of basic principles, quantitative measurement, the emerging technology and artificial intelligence. The basic principles of LSCI including

979-8-3503-9956-1/22/$31.00 ©2022 IEEE
DOI 10.1109/EIECT58010.2022.00077

speckle theory, contrast analysis and blood flow imaging methodology are described in Section 2. To make LSCI a quantitative blood flow imaging instrument, several attempts have been made such as elimination of static scattering, speckle averaging and reduction of system noise. These can be found in section 3. Multiple exposure laser speckle contrast imaging (MELSCI) utilizing a wide range of exposure times to calibrate LSCI like LDI (laser Doppler blood flow imaging) is also elaborated in Section 3. Further optimization of LSCI using machine learning is discussed in Section 4. Section 5 describes conclusions and future work.

II. Principles of laser speckle contrast imaging

A. Speckle theory

Laser speckle is an interference phenomenon when coherent light irradiates a rough surface or propagates within a medium containing scattering particles[1, 26-27]. Depending on the paths of the interfered light, bright or dark regions are formed when the light waves superimpose. If the light waves arrive in phase, a bright spot is observed. If the light waves arrive with opposite phase, the amplitude cancels each other, resulting in dark spots. Because the light intensity at any point is determined by the superposition of all light arriving at the point, bright spots and dark spots are randomly distributed, and this is known as a laser speckle pattern[26]. When the illuminated surface moves or there are moving scatterers such as particles in fluid, the speckle intensity randomly fluctuates providing a time-varying speckle pattern. The time-varying speckle is identical to the light intensity fluctuation due to the Doppler effect, as they are two different descriptions of the same process[26]. If using a time-integrating camera to acquire the time-varying speckle pattern, it is the integrated intensity during the exposure time that is recorded. The decorrelation time (τ) can be used to quantify the dynamics of the scatterers. Mathematically, this factor represents the autocorrelation function width and is used to describe the delays. As a result, the imaged speckle pattern is blurred by the integration when the speckle varies. Goodman[28] quantifies this blur with speckle contrast, as laser speckle is a random phenomenon, it can be described statistically. Speckle contrast is defined as the ratio of standard deviation to average intensity:

$$K = \sigma / \langle I \rangle = \sqrt{\left\langle \left(I - \langle I \rangle \right)^2 \right\rangle} / \langle I \rangle \tag{1}$$

Where K is the speckle contrast, σ is the standard deviation of speckle intensity, $\langle I \rangle$ is the average value of speckle intensity. For an ideal surface, the standard deviation of the intensity change in the speckle pattern is equal to the average intensity[28]. But in fact, the standard deviation in a speckle pattern is usually less than the average intensity, this means that the contrast is always less than 1 ($0 \le K \le 1$).

B. Measurement on blood flow based on speckle analysis

Stern[29] realized that time-varying speckle could be used to measure the fluctuation caused by blood flow. The fluctuating speckle pattern due to the motion of red blood cells (RBCs) cause a reduction of speckle contrast which can be used to indicate the velocity. It is worth noting that the majority of the detected light propagates in superficial tissue and only a small percentage is scattered by the moving RBCs. Therefore, laser speckle contrast imaging is often used for skin microcirculation imaging.

The scattering particles due to blood flow, RBCs, are distributed over a range of velocities from 0 mm/s to 2 mm/s[30]. Faster moving scatterers result in higher frequency of speckle fluctuation and vice versa. Consequently, the relationship between intensity and decorrelation time (τ) can be described by an autocorrelation function. The shorter the correlation time, the faster the intensity changes, indicating faster blood flow velocity. According to Goodman's early work on speckle statistics [28], the spatial variance of the intensity of a time-varying speckle pattern σ^2, can be linked with the autocovariance of the intensity fluctuations C_t, by

$$\sigma_s^2(T) = \frac{1}{T}\int_0^T C_t(\tau)\,d\tau \tag{2}$$

Where T is the exposure time, τ is the speckle correlation time. Since the correlation time is inversely proportional to the velocity, Eq.(2) presents an approach to relate the velocity to the speckle spatial variance. To make use of Eq.(2), the true velocity distribution should be known in advance. In general, either a Lorentzian or Gaussian distribution is applied to relate contrast to correlation time. Assuming a Lorentzian velocity distribution, Fercher and Briers[1] rephrased Eq.(2) to

$$K = \frac{\sigma}{\langle I \rangle} = \left[\frac{\tau_c}{2T} \left\{ 1 - \exp\left(\frac{-2T}{\tau_c} \right) \right\} \right]^{\frac{1}{2}} \tag{3}$$

Where T is the photodetector exposure time. In general, the exposure time T is much longer than the correlation time τ_c, so the speckle contrast K has a linear relationship with τ_c[27]. The relationship between the scatterer velocity V and the time of decorrelation is usually expressed as:

$$V = \frac{\lambda}{2\pi\tau_c} \tag{4}$$

Where λ is the wavelength of illumination. The scatterer velocity V is inversely proportional to the time autocorrelation τ_c. Since the autocorrelation is directly proportional to the speckle contrast, the velocity is inversely proportional to the contrast.

C. Contrast analysis domain

As mentioned above, dynamic speckle can affect the contrast, and contrast can be associated with velocity. Therefore, the traditional method of velocity estimation using LSCI is to calculate contrast. There are three commonly used contrast analysis methods: spatial contrast analysis; temporal contrast analysis; and spatio-temporal contrast analysis. Although they have computational similarities, they are characterized differently.

Spatial contrast analysis is the initial methodology of LSCI and firstly proposed by Briers and Webster[31]. In operation,

non-overlapping sliding of the windows with typical size of 3×3, 5×5 or 7×7 pixels are adopted to carry out the statistical calculation according to Eq.(1) The advantage is that it can provide blood perfusion imaging in real time since only one frame is required for processing. However, it is at the expense of spatial resolution [32]. The speckle average caused by improper speckle size will bring large contrast error and significantly affect the imaging accuracy.

Unlike spatial contrast analysis shown in Fig. 2(a), the temporal speckle contrast method introduced by Cheng et al.[33] is calculated from multiple frames shown in Fig. 2(b). For processing one temporal contrast, the pixels in the same position of a series of frames are involved in the calculation which is defined as the same as Eq.(1). Consequently, it is the temporal equivalent of the spatial contrast. In comparison to spatial contrast analysis, Wang et al.[34] have found that, temporally processing immunizes against static scattering (such as a skull that is stationary relative to moving RBCs) which is the reason of underestimation in spatial contrast. Although temporal contrast analysis has many benefits for such a speckle contrast-based blood flow imaging system, limitations are recognized as well. Firstly, temporal contrast analysis improves the spatial resolution at the expense of temporal resolution which is the most important feature of such speckle contrast-based systems. Typically, imaging speed for the temporal contrast system is a few tens slower than the system based on spatial contrast. Secondly, Cheng[33] found that no flow and very high flow both give a zero-contrast map, which means neither static nor fully developed speckle patterns can be mapped into contrast by using the temporal contrast method. To overcome these disadvantages, a new processing scheme combining these two speckle contrast methodologies was introduced to fulfil different trade-offs between the spatial resolution and the temporal resolution.

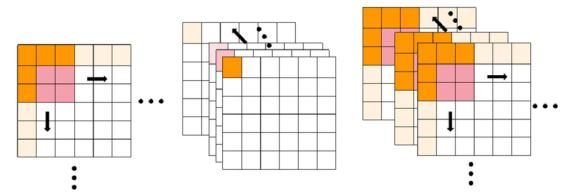

(a)Spatial contrast (b)Temporal contrast (c)Spatio-temporal contrast

Fig. 2 Schematic diagram of three contrast calculation methods. Beige indicates image pixels. Pink 3×3 window is the calculation boundary of primary contrast. The black arrow indicates the calculation direction.

Spatio-temporal contrast analysis is a combination of spatial contrast and temporal contrast and typically compromises between the spatial resolution and the temporal resolution [2, 35-37]. For example, Duncan and Kirkpatrick[35] employed 3×3 local pixels in 15 adjacent frames to calculate the contrast. Dunn et al. [2] calculated the local contrast in spatial domain and averaged temporally. Qiu et al. [36] found that both spatial and temporal dimensions will affect the average value of contrast[37]. proposed anisotropic LSCI. This spatio-temporal scheme takes the advantage of high CNR (Contrast-to-Noise Ratio) by introducing anisotropic pixels. In this scheme the local contrast is calculated along the direction of blood flow, and a few frames are utilized to keep the sub-window in the spatio-temporal domain. In operation, the direction of blood flow for each pixel (primary pixel) in the ROI (region of interest) is determined. Then a pixel group of the spatio-temporal neighborhood is extracted only in the blood flow direction. For each primary pixel, the speckle contrast is calculated as the ratio of the standard deviation and the average value of all pixels in the anisotropic neighborhood.

D. Laser speckle contrast blood flow imaging system

Typically, Laser speckle contrast imaging applies the spatial statistics of time-accumulated dispersed speckle. This was originally reported by Briers for measurement of retinal blood flow[1]. During imaging, the motion of the scattered particles causes the intensity of each speckle to fluctuate, so averaging the speckle intensity within the exposure time will reduce the speckle contrast. According to the relationship between speckle contrast and correlation time Eq. (3), it can be inferred that there must be a relationship between flow velocity and contrast reduction.

In 1996, David and Webster proposed the first digital LSCI based on time-varying laser speckle phenomenon[32]. Afterwards, some researchers have further studied and improved LSCI technology by introducing either new hardware or processing schemes [39-42]. Liu et al.[39] introduced GPU (Graphics Processing Unit) for data processing and achieved faster imaging at high resolution which is hard to be achieved with a CPU (Central Processing Unit) in general PCs. Yang et al.[40] increased the processing speed further by presenting a novel algorithm that employs the NVIDIA Compute Unified Device Architecture (CUDA) platform to perform LSCI processing in the GPU. This enables acquisition of 10 raw speckle images every second at high resolution (1392×1024). Richards et al. [41] used inexpensive aspheric lenses, a webcam and a laser pointer to build a low-cost, compact-setup LSCI system ($90, 5.6 cm length, 25g). Jiang et al.[42] proposed a real-time LSCI processing scheme based on a field programmable gate array (FPGA), which can process 85 LSCI images every second at resolution of 640×480 pixels. Recently, multi-tap CMOS sensor has been applied in this field. Sivakumar et al.[43] applied a low-cost multi-tap CMOS image sensor to build up a low-power and cost-effective MELSCI system. Kagawa[44] developed an imaging system based on multi-tap CMOS pixel which is modified to achieve synchronous active lighting and coded exposure at the expenses of increment of dark current and sensitivity reduction. Although the single exposure LSCI is continuously optimized in terms of processing speed and imaging quality, it's recognized as having the advantage of system simplicity.

III. Principles of laser speckle contrast imaging

LSCI as a full-field, non-invasive blood perfusion imager is widely applied in both research investigations and clinical studies. Whereas the application is limited as it is lack of linearity and unable to provide quantitative blood perfusion measurement. This is because of either presence of static scatterings and noise, the effect of speckle averaging or the

uncertainty of speckle model. Efforts have been continuously made to improve it as a quantitative instrument.

A. Presence of static scatterers

Li et al [45] suggested to use temporal contrast analysis instead of spatial contrast analysis. As the contrast produced by static scatterers does not change with time, they claimed that the calculation method in temporal domain could effectively reduce the error caused by static scatters. Zakharov et al [46] introduced a robust contrast model to separate the effect of dynamic and static scattering based on the statistical speckle model proposed by Fercher and Briers[47]. In 1981, Fercher and Briers used the electric field autocorrelation function $g_1(\tau)$ to quantify the temporal fluctuation of speckle. According to the Siegert relation, the intensity autocorrelation function $g_2(\tau)$ can be recorded by Eq.(5).

$$g_2(\tau) = 1 + \beta |g_1(\tau)|^2 \tag{5}$$

Where β is the normalization factor indicating the speckle averaging effect. Fercher and Briers[47] calculated the contrast of the ideal speckle model on the assumption that $\beta = 1$.

$$K(T, \tau_c) = \left(\frac{1 - e^{-2x}}{2x}\right)^{1/2} \tag{6}$$

Where $x = T/\tau_c$, T is the exposure time of camera, and τ_c is the correlation time. Considering the average scattering effect Bandyopadhyay[48] proposed a more robust model as

$$K(T, \tau_c) = \left(\beta \frac{-e^{-2x} - 1 + 2x}{2x^2}\right)^{1/2} \tag{7}$$

However, this equation can't be used in the presence of static scatterers because the use of Siegert relationship is under the assumption of Gaussian distribution. In the presence of static scatterers, the intensity has an extra static contribution, as a result it no longer satisfies Gaussian distribution. Zakharov et al [46] proposed a modified equation with the absence of static scatterers.

$$\begin{aligned} K^2 &= \frac{2\beta}{T} \int_0^T \left[(1-\rho)|g_{1d}(\tau)| + \rho\right]^2 (1 - \tau/T) d\tau \\ &= (1-\rho)^2 K_{2d}^2 + 2\rho(1-\rho) K_{1d}^2 + \beta\rho^2 \end{aligned} \tag{8}$$

Where $\rho = \langle I_s \rangle / (\langle I_s \rangle + \langle I_d \rangle)$, $\langle I_s \rangle$ is the non-fluctuating static part and $\langle I_d \rangle$ is the dynamic part. K_{2d} and K_{1d} represent the contrast of the dynamic intensity and the dynamic field are given as:

$$\begin{aligned} K_{2d}^2 &= \frac{2\beta}{T} \int_0^T |g_{1d}(\tau)|^2 (1 - \tau/T) d\tau \\ K_{1d}^2 &= \frac{2\beta}{T} \int_0^T |g_{1d}(\tau)| (1 - \tau/T) d\tau \end{aligned} \tag{9}$$

To use Eq.(8), a setup with a high-frame rate camera and a high-power laser source is crucial to ensure sufficient photons are collected in a short exposure time.

In terms of noise, Wang et al. [34] have used correction methods to eliminate errors of static scatterers and noise. They advocated utilizing K2 as speckle contrast instead of traditional K. When K2 is applied, it is shown great improvement on the linear range of the flow index covering the whole range from 0 to 40 mm/s.

B. Speckle averaging effect

In practice, in addition to static scatterers and noise, another factor that affects the accuracy of the calculation is the speckle size. The speckle size is a key parameter which is typically defined as the number of pixels occupied by a single imaged speckle[49]. If the speckle size is smaller than a pixel, that is, a pixel contains multiple speckles, spatial averaging effect of the finite pixels occurs, resulting in the decrease of speckle contrast [28]. Goodman defines the decreased contrast as Eq.(10) [28].

$$K = 1/\sqrt{n} \tag{10}$$

Where n is the number of coherence region inside the measurement area.

In a lens system, speckle size depending on the wavelength of irradiation light and the optic setup [51] is calculated by Eq.(11)[49].

$$d_{\min} = 1.2(1 + M)\lambda f/\# \tag{11}$$

Where $d_{\min}$ is the minimum speckle diameter, M is the magnification of the imaging system, and $f/\#$ is the f-number of the lens which can be straightforwardly changed by adjusting the aperture size of the camera. In consideration of Nyquist sampling criterion, Kirkpatrick et al. [50] advise to match the speckle size as twice as the pixel size . Accordingly, Eq.(11) is modified to

$$d_{\min} = 2.4(1 + M)\lambda f/\# \tag{12}$$

In practice, Eq.(11) is more commonly applied as some believe that in order to obtain good statistics and small errors, the speckle size should equal to the pixel size [52-53].

As mentioned above, if the speckle is smaller than a pixel, the speckle contrast K is underestimated due to speckle averaging effect. On the contrary, an increase of speckle size will lead to loss on spatial resolution and the reduction of speckle contrast due to the drop of standard deviation. Therefore, it is necessary to make a tradeoff optimizing the speckle size. Early LSCI literature showed that 1 pixel / speckle was always used as the speckle size [52, 54]. However, Kirkpatrick et al. [50] have proved that 1 pixel/speckle will cause speckle under sampling, making the maximum K value about 0.7, which is 30% less than the asymptotic value of 1.0 when the speckle pattern is fully sampled. They proposed that spatial aliasing under the condition of negative exponential distribution should be avoid by satisfying Nyquist sampling theorem. As a result, they advise the optimal speckle size must be greater than twice the size of the detector pixel. However, the reduction of the maximum contrast kmax due to the spatial averaging remains even the speckle size is perfectly matched.

Thompson and Andrews [53] proposed a linear system correction parameter $\beta = 1/K_{\max}$ ($K_{\max} < 1$) to eliminate the error. Thompson et al.[55] demonstrated the effectiveness of the linear correction even in the present of static scattering speckles and background illumination noise.

C. Exposure time

In addition, the contrast of the laser speckle depends on both the velocity of the blood flow and the exposure time. In a very short exposure time, the laser speckle is quickly imprinted to form a high-contrast speckle pattern. While a longer exposure time will make the speckle intensity averaged and form a low-contrast speckle pattern. Yuan et al.[56] studied the relationship between sensitivity, noise and camera exposure time by imaging the speckle contrast changes on brain after electrically stimulating rat front paws. The results showed that 5 ms was the optimal exposure time for imaging changes of rat's cerebral blood flow induced by stimulation.

Since 2008, Pathasarathy et al. [57] firstly proposed Multi-Exposure Laser Speckle Contrast Imaging (MELSCI) instrument that has potential to obtain quantitative baseline flow measurements, more research has been carried out in this field [58-61]. This method effectively changes the speckle exposure time T by fixing the exposure time of the actual camera and gating a laser diode during each exposure, and then obtain speckle images at multiple exposure times. The MELSCI calculation model proposed by Pathasarathy et al. [57] is shown in Eq. 13.

$$K(\tau_c) = \left\{ \begin{array}{l} \beta\rho^2 \dfrac{e^{-2x} - 1 + 2x}{2x^2} + \\ 4\beta\rho(1-\rho)\dfrac{e^{-x} - 1 + x}{x^2} + v_{ne} + v_{noise} \end{array} \right\}^{1/2} \quad (13)$$

Where $x = T/\tau_c$, T is the camera exposure time, and τ_c is the correlation time, β is the normalization factor indicating the speckle averaging effect, $\rho = \langle I_s \rangle / (\langle I_s \rangle + \langle I_d \rangle)$, $\langle I_s \rangle$ is the non-fluctuating static part and $\langle I_d \rangle$ is the dynamic part. v_{noise} is the constant variance due to experimental noise and v_{ne} is the constant variance due to non-ergodic light.

The above formula is the contrast calculation model of Lorentz distribution, and Parthasarathy et al. [38] also lists the calculation model under assumption of Gaussian distribution.

$$K(T, \tau_c) = \left\{ \begin{array}{l} \beta\rho^2 \dfrac{e^{-2x} - 1 + \sqrt{2x}\, xerf(\sqrt{2}x)}{2x^2} + \\ 2\beta\rho(1-\rho)\dfrac{e^{-x} - 1 + \sqrt{\pi}\, xerf(x)}{x^2} + v_{ne} + v_{noise} \end{array} \right\}^{1/2} \quad (14)$$

Subsequently, the model of Eq.(13) was extended by Kazmi et al. [60], as shown in Eq.(15) with a clearer definition of v_{ne}.

$$K^2(T) = \beta \frac{\rho^2\tau^2}{2T^2}\left[e^{-\frac{2T}{\tau}} - 1 + \frac{2T}{\tau}\right] + \beta\frac{4\rho(1-\rho)\tau^2}{T^2}\left[e^{-\frac{T}{\tau}} - 1 + \frac{T}{\tau}\right] + \beta(1-\rho)^2 + v_{noise} \quad (15)$$

In-vivo studies have shown that compared with single exposure LSCI measurement Eq.(7), MELSCI Eq.(15) can significantly improve the accuracy of measured flow dynamics due to global and local flow disorders in acute and chronic environments [36]. In addition, Nadort et al. [58] applied Sidestream Dark Field (SDF) to MELSCI and obtained the speckle decorrelation time relation to the microcirculation flow. It enables direct comparison to the flow rate and quantitative detection of microcirculation. Atchia et al. [59] proposed a novel multi-exposure LSCI that using the short transient times of VCSELs (Vertical cavity surface emitting lasers), which simplified the MELSCI imaging system and corrected the images of high-speed fluids and static scatterers. Kazmi et al. [60] used a new algorithm called looping leave-one-out (LOO) to identify exposure subsets. With this setup, the optimal camera exposure durations can be determined. However, because of the wide extension of exposure time, adjustment of illumination intensity is required. This introduced system complexity. Sun et al. [61] integrated the MELSCI with a high frame rate CMOS imaging sensor chip and implemented it using a field programmable gate array (FPGA). In this system, LSCI images are acquired at a fixed exposure time, multiple exposure time are achieved by accumulating several adjacent frames. Recently, by quantifying and comparing the contribution of noise to speckle contrast, Chammas & Pain [62] found that the method of synthetic exposure images generated by the sum of continuous frames obtained within 1ms exposure time is easy to realize and should be applied in clinic.

D. The relationship between LSCI and LDI

Another well used non-invasive blood flow imaging technology is laser Doppler blood flow imaging (LDI). Although LSCI and LDI have been developed separately, there are similarities that both detect and process the wave interference of coherent light scattered by moving red blood cells (RBCs). LSCI is dependent on the processing that relates spatial/temporal speckle contrast to a suitable model of blood flow. LDI is alternatively based on the well-known Doppler effect which occurs when light is scattered by moving RBCs. Because of the difference between the processing schemes, they are characterized differently. LDI is featured as a quantitative blood flow imaging instrument at the expense of imaging speed and system complexity. LSCI, on the contrary, possessing short blood flow image acquisition time and simple system set up, lacks accuracy and linearity to blood flow [63-64].

The relationship between LSCI and LDI has been discussed in many papers. Some researchers have compared LDI and LSCI [64-68], and were devoted to improving the imaging accuracy of LSCI to LDI. Forrester et al. [64] and Stewart et al. [65] experimentally compared the performance of LDI and LSCI and proved that the LSCI has relatively better temporal and spatial resolution, but it is far inferior to LDI in terms of imaging accuracy. As a strong positive correlation between these two imaging results was observed, the least square was applied to correlation. Some studies [66-68]. compared LDI and LSCI based on in vivo measurements. Millet et al. [66] tested the occlusion and congestion of the human forearm and found that LDI and

LSCI are linearly related to the measurement of perfusion. On the contrary, Tew et al. [67] and Humeau-Heurtier et al. [68] concluded differently in similar measurements as LSCI is unable to provide linear measurement like LDI and a power function can more accurately link LSCI to LDI. As they concluded, LSCI is more sensitive to changes in red blood cell velocity than red blood cell concentration [67]. However, because of the different subjects and other objective factors, the coefficient of the power functions are not the same. Sun et al. [30] compared the LSCI and LDI using same photons captured using a high frame rate camera but processed using LSCI and LDI algorithms. The results show that LSCI is related to exposure time. The longer the exposure time, the more sensitive to low speed, and vice versa. Meanwhile, they can be classified and linked by two cases, namely, the linear relationship in the case of short exposure time and the power function relationship in the case of long exposure time, which is usually used for blood flow imaging. Parthasarathy et al. [57] proposed a speckle model for MELSCI, which can distinguish flows with static scatterers. This model was subsequently corrected by Kazmi et al. [60]. However, the computational requirements of this model are too high to be suitable for real-time application. In addition, Thompson and Andrews [53] concluded that the multi-exposure speckle contrast measurements can recover the same spectral information as laser Doppler measurements using both simulated speckle data and experimental measurements on Brownian motion and skin perfusion. Recently, Kelsey et al. [69] studied the reproducibility of reflex cutaneous vasoconstriction response by using LSCI in human experiments and proved that LSCI has stronger test-retest reproducibility and reliability than LDI, so it may be more suitable for longitudinal evaluation.

IV. Artificial Intelligent-based LSCI

With the rapid development of machine learning, this cutting-edge technology has been applied to a wide range of applications including LSCI. In 2019, Fredriksson et al. [70] demonstrated that multi-exposure laser speckle contrast imaging can perform LDI-like measurement by utilizing machine learning. In this study, a set of 100,000 simulated data was utilized. An ANN (artificial neural network) was trained with input of contrasts from 7 different exposure times and traditional LDF (laser Doppler blood flowmetry) perfusion as outputs. The results showed high accuracy with correlation coefficient R = 1.000 for noise-free data and R = 0.993 for noisy data. Because significant errors are presented when stochastic noise is only added to evaluation set (shown in table 1), they claimed that it is essential to account for noise when training the ANN-MELSCI model. This is instructive for applying machine learning in practice as noise is non-ignorable in reality. An in vivo measurement of post congestion experiment was also conducted to evaluate the performance of ANN-MELSCI model. Feasibility of using ANN-MELSCI to replace LDI is demonstrated by both time-varying perfusion estimates and spatial maps of perfusion with high accuracy of R = 0.995. It is worth noting that the ANN-MELSCI model is able to perform high-quality in-vivo measurement even though it is established using simulated speckle data. This illustrates the great flexibility of machine learning applied to LSCI. However, in order to ensure the effectiveness in practice, the modeling data of the Doppler histogram needs to cover the whole frequency spectrum of blood flow changes which is typically 20 Hz ~ 20 kHz [70]. As the LDI data is system dependent, this means the accuracy of the ANN-MELSCI model varies with bandwidth of frontend, system noise and optical setup. A high-speed camera is crucial in this system.

Table 1 Different noise adding methods in training set and test set are used to compare the influence of random noise on system training [70]

	Training set	Evaluation set	R[-]	RMSa(PU)	RMSr(%)
ANN	Added noise	Added noise	0.993	9.5	19
	No noise	Added noise	0.090	12,300	132,866
	Added noise	No noise	0.997	6.5	11
LDF from speckle simulations			0.997	6.4	9.9

Deep learning is also applied to improve LSCI imaging accuracy by denoising. The feed-forward denoising convolutional neural network (DnCNN) has superior performance in image denoising. Cheng[71] et al. applied it to denoise LSCI original speckle images. However, it performs poorly in learning owing to the inhomogeneous noise distribution. Therefore, the training was carried out in the log-transformed domain, which achieves an improvement of 5.13 dB in the peak signal-to-noise ratio (PSNR). In order to maintain the real-time performance of LSCI, a dilated residual learning network with skip connections (DRSNet) was further proposed, which achieved approximately 2.5 times faster than DnCNN.

In addition, Stebakov et al.[72] trained a feed-forward ANN using LSCI flow data of 0-2mm/s in glass capillaries. The accuracy of this model in identifying flow rate based on images is 10% higher than that of experts, which reflects the advantages of deep learning over the human eyes. However, it uses classification recognition to predict the flow rate, but the flow rate is a continuous index related to time. The classification problem can only cover some discrete flow rates with large characteristics, which is far from enough to be applied in clinical practice. Therefore, it should be regarded as a regression problem to expand the prediction range and continuity.

K-means clustering[73], as a typical machine learning method, is also applied to the calculation of LSCI contrast, which determines the localization of blood vessels largely. So it improves the ability of LSCI to locate blood vessels, but it is only applicable when the blood vessels and tissue regions are well separated from each other.

These results demonstrate the high potential of utilizing machine learning in LSCI. This is because the ‘black box’ eliminates the influence of uncertain factors in comparison to the traditional speckle-based methodologies. These uncertainties are introduced because of either the speckle theory used in LSCI are derived under some assumptions and

approximations or the difficulties that accurately describe properties of light passing through e.g. static scattering, speckle averaging effect, imaging noise.

As multi-exposure LSCI has been demonstrated to be a quantitative blood flow measurement like LDI, it is worth trying to establish the mapping model between speckle contrast under single exposure and speckle decoherence time under multiple exposure. This model could be set up using quantitative experimental data to improve the accuracy of training. In this way, measurement of LSCI could be improved without increasing system complexity and sacrificing imaging speed. We proposed reinforcement learning with convolutional neural network (CNN) to achieve this, as shown in Fig. 3. In operation, a CNN-LSCI model could be set up by using simulated speckle data. Reinforcement learning is, thereafter, performed based on quantitative-controlled experimental data. For example, a custom designed tissue phantom mimicking RBCs flowing under skin could be adopted. This tissue phantom is composed of a servo motor, a uniform diffuse reflection plate and a frosted glass reflector. The motor drives the animation reflector to rotate behind the frosted glass at a certain angular speed, so as to simulate the red blood cells flowing under the epidermis in human tissue. The linear speed on the diffuse reflection plate is proportional to the radius, producing controlled velocity distribution. In this way, performance could be further improved by accounting for the system noise and optical noise in reinforcement learning. Because the experimental data generated by rotating scattering plate is quantifiable, system evaluation could be undertaken in comparison to actual speed, realizing quantitative measurement. More details will be described in our future publication.

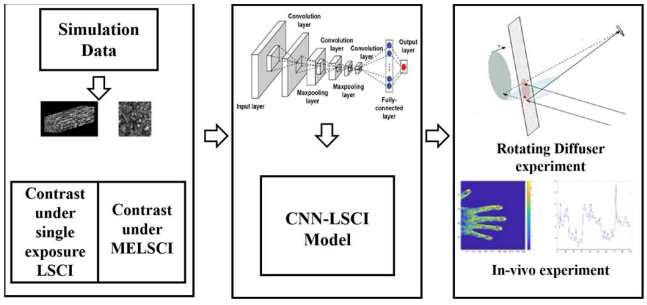

Fig. 3 Schematic diagram of proposed scheme. A CNN-LSCI model is set up by using simulated speckle data. Reinforcement learning is performed based on quantitatively controlled experimental data. The data is generated by imaging a custom designed tissue phantom mimicking RBCs flowing under skin. In this way, the CNN-LSCI model could be further enhanced by accounting for the system noise and optical noise. The controlled data enable the CNN-LSCI model to be evaluated to actual velocity, realizing quantitative analysis

V. Conclusions

LSCI has become a prevalent noninvasive blood flow imaging technology in recent years. It benefits from fast imaging speed, high resolution and system simplicity and has been widely used in clinics and research. However, it lacks quantitative measurement, therefore, continuous efforts have been made to improve imaging accuracy and measurement linearity of LSCI. New speckle models, multi-exposure imaging (MELSCI) and artificial intelligence methods have all been introduced. This paper reviews LSCI from imaging principle, basic theory and has summarized the effects of speckle size, analysis domain and exposure time. Different algorithm models, the relationship between LSCI and LDI and application of machine learning in LSCI are discussed as well. The application of machine learning shows a great potential to improve LSCI as an LDI-like instrument. It is of great interest to calibrate single exposure laser speckle contrast imaging to multiple exposure laser speckle contrast imaging by using machine learning.

The future development of LSCI is related to its current limitations of absolute estimation of velocity and the depth of perfusion measurement. The absolute estimation of velocity determines the quantitative measurement of perfusion which are affected by multiple factors, including static scatterers, spatial average of speckle and measurement noise. This can be further improved by optimizing the speckle algorithm and updating the hardware. The depth of measurement is determined by the property of coherent light. Combination with other optical methods such as near-infrared diffuse correlation spectroscopy can be introduced to detect deeper blood perfusion[74]. In addition, the application of machine learning can optimize perfusion measurement further, that using simple databases to achieve quantitative measurement in high accuracy.

Acknowledgments

The authors acknowledge the support from the program of China Scholarship Council (CXXM20210004).

References

[1] Briers, J.D., Fercher, A.F. (1982) Retinal Blood Flow Visualization by Means of Laser Speckle. Invest Ophth Vis Sci., 22: 255-259.

[2] Dunn, A.K., Bolay, H., Moskowitz, M.A., Boas, D.A. (2001) Dynamic Imaging of Cerebral Blood Flow Using Laser Speckle. J Cerebr Blood F Met. ,21: 195–201.

[3] Li, L., Liu, S., Miao, P.(2020) Real time evaluation of mouse carotid thrombosis model by laser speckle imaging. Industrial Control Computer., 33: 43-44.

[4] Liu, P., Tang, Y., She, D., Ma, L., Pan, L., He, C. (2020) Effect of glibenclamide on cerebral microcirculation after SAH in mice monitored by laser speckle imaging. Chinese Journal of Clinical Neurosurgery., 25: 538-541.

[5] Zhao, Y., Xue, Y., Zhang, Y., Weitao, L.I., Qian, Z. (2019) Development of Blood Flow and Oxygen Monitoring System for Mice Based on Laser Speckle and Spectrum. Chinese journal of medical instrumentation., 43: 1-4.

[6] Couturier, A., Bouvet, R., Cracowski, J.L., Roustit, M., Kotzki, S. (2020) Laser speckle contrast imaging as a better tool to access the cutaneous microcirculation: Reproducibility and comparison to laser Doppler imaging in animal models. Archives of Cardiovascular Diseases Supplements., 12: 208-209.

[7] Sorelli, M., Francia, P., Bocchi, L., Bellis, A.D., Anichini, R. (2019) Assessment of cutaneous microcirculation by laser Doppler flowmetry in type 1 diabetes. Microvasc Res., 124: 91-96.

[8] Yu, Q., Yu, Y., Zhong, J., Lei, H., Wang, P. (2018) Monitoring and evaluation system of blood microcirculation after finger replantation based on laser speckle imaging. In: The 17th Chinese optical testing academic exchange.ChangChun.265.

[9] Jiang, M.J., Chu, Z.G., Xie, Q.H., Huang, W.W., Ruan, J.J., Xie W.G. (2016) Application of laser speckle perfusion imaging in predicting

wound healing time of burn patients. Chinese Journal of burns., 32: 721-724.

[10] Jayanthy, A.K., Sujatha, N., Reddy, M.R., Narayanamoorthy, V.B. (2014) Non invasive blood flow assessment in diabetic foot ulcer using laser speckle contrast imaging technique. Proc. SPIE 8952, Biomedical Applications of Light Scattering VIII.,89521D.

[11] Mirdell, R., Farnebo, S., Folke, S., Tesselaar, E. (2020) Using blood flow pulsatility to improve the accuracy of laser speckle contrast imaging in the assessment of burns - ScienceDirect. Burns., 46: 1398-1406.

[12] Jan, S.N., Khan, F.A., Bashir, M.M., Nasir, M., Ansari, H.H., Shami, H.B., Nazir, U., Hanif, A., Sohail, M. (2018) Comparison of Laser Doppler Imaging (LDI) and clinical assessment in differentiating between superficial and deep partial thickness burn wounds - ScienceDirect. Burns., 44: 405-413.

[13] Wang, Y., Louie, D.C., Cai, J., Tchvialeva, L., Lee, T.K. (2021) Deep learning enhances polarization speckle for in vivo skin cancer detection. Opt Laser Technol., 140: 107006.

[14] Zeng, W., Lu, T., Liu, Z., Xu, Q., Yao, F. (2021) Research on a laser ultrasonic visualization detection method for human skin tumors based on pearson correlation coefficient. Opt Laser Technol., 141: 107117.

[15] Zheng, K.J., Middelkoop, E., Stoop, M,, Zuijlen, P.P.M., Pijpe, A. (2021) Validity of laser speckle contrast imaging for the prediction of burn wound healing potential. Burns., 48: 319-327.

[16] Elmasry, M., Mirdell, R., Tesselaar, E., Farnebo, S., Sjoberg, F., Steinvall, I. (2019) Laser speckle contrast imaging in children with scalds: Its influence on timing of intervention, duration of healing and care, and costs. Burns., 45: 798-804.

[17] Philimon, S.P., Huong, A. (2021) Laser Speckle Integrated Multispectral Imaging System for In-Vivo Assessment of Diabetic Foot Ulcer Healing: A Clinical Study. IEEE Access., 9: 23726 - 23736

[18] Kataoka, K., Kase, S., Noda, K., Ishida, S. (2020) Laser Speckle Flowgraphy Findings in a Patient with Choroidal Macrovessel. Ophthalmology Retina.,15:172-174.

[19] Hanazaki, H., Yokota, H., Aso, H., Yamagami, S., Nagaoka, T. (2021) Evaluation of ocular blood flow over time in a treated retinal arterial macroaneurysm using laser speckle flowgraphy. American Journal of Ophthalmology Case Reports., 21: 101022.

[20] Fadel, B.M., Pibarot, P., Kazzi, B.E., Al-Admawi, M, Galzerano, D., Alhumaid, M., Alamro, B., Mahjoub, H., Echahidi, N., Mohty, D. (2021) Spectral Doppler Interrogation of the Pulmonary Veins for the Diagnosis of Cardiac Disorders: A Comprehensive Review. J Am Soc Echocardiog., 34: 223-236.

[21] Jia, X., He, J., Lu, H., Young L., Tong, S. (2018) Real time cerebral blood flow monitoring by laser speckle contrast imaging after cardiac arrest with targeted temperature management. Ann Phys Rehabil Med., 61: e425.

[22] Wang, C., Xian, L., Chen, X., Li, Z., Wang, S. (2020) Visualization of cortical cerebral blood flow dynamics during craniotomy in acute subdural hematoma using laser speckle imaging in a rat model. Brain Res., 1742: 146901.

[23] Takeshima, Y., Miyake, H., Nakagawa, I., Motoyama, Y., Park, Y.S., Nakase, H. (2015) Visualization of Regional Cerebral Blood Flow Dynamics during Cortical Venous Occlusion using Laser Speckle Contrast Imaging in a Rat Model. J Stroke Cerebrovasc., 24: 2200-2206.

[24] Liu, H., Chen, D., Liu, S., Jia, J., Miao, P. (2020) Hand function rehabilitation evaluation system and software for stroke patients based on laser speckle flow imaging. Industrial Control Computer., 33: 20-21+24.

[25] Wu, D., Yao, K., Guan, K., Fu,W., Sun, J., Guo, Y., Wang, C. (2020) Cerebral blood flow analysis based on laser speckle contrast imaging technology. Optical precision engineering., 28: 2411-2420.

[26] Briers, J. D. (2001) Laser Doppler, speckle and related techniques for blood perfusion mapping and imaging. Physiol Meas., 22: R35.

[27] Li, C., Chen, W., Jiang, J., Fan, Y., Yang, J., Xu, K. (2018) Research progress of laser speckle contrast blood flow imaging. China laser., 45: 92-101.

[28] Goodman, J.W. (1963) Statistical Properties of Laser Speckle Patterns. Topics in Applied Physics. In: Dainty, J.C. (Eds.), Laser Speckle and Related Phenomena. Springer, Berlin, Heidelberg. 9-75.

[29] Stern,D.M. (1975) In vivo evaluation of microcirculation by coherent light scattering. Nature., 254: 56-58.

[30] Sun, S., Hayes-Gill, B.R., He, D., Zhu, Y., Huynh, N.T., Morgan, S.P. (2016) Comparison of laser Doppler and laser speckle contrast imaging using a concurrent processing system. Opt Laser Eng., 83: 1-9.

[31] Briers, J.D., Webster, S. (1996) Laser speckle contrast analysis (LASCA): a nonscanning, full-field technique for monitoring capillary blood flow. J Biomed Opt., 1: 174-179.

[32] David, A.B., Andrew, K.D. (2010) Laser speckle contrast imaging in biomedical optics. J Biomed Opt., 15:011109.

[33] Cheng, H., Luo, Q., Zeng, S., Chen, S., Cen, J., Gong, H. (2003) Modified laser speckle imaging method with improved spatial resolution. J Biomed Opt., 8: 559-64.

[34] Wang, C., Cao, Z., Jin, X., Lin, W., Xu, M. (2019) Robust quantitative single-exposure laser speckle imaging with true flow speckle contrast in the temporal and spatial domains. Biomed Opt Express., 10: 4097.

[35] Duncan, D.D., Kirkpatrick, S.J. (2008) Spatio-temporal algorithms for processing laser speckle imaging data. In: Conference on Optics in Tissue Engineering and Regenerative Medicine. San JoseCA. 20080120-21.

[36] Qiu, J., Li P., Luo W., Wang, J., Zhang, H., Luo, Q. (2010) Spatiotemporal laser speckle contrast analysis for blood flow imaging with maximized speckle contrast. J Biomed Opt., 15:016003.

[37] Rege, A., Senarathna, J., Li, L., Thakor, N.V. (2012) Anisotropic Processing of Laser Speckle Images Improves Spatiotemporal Resolution. IEEE Transactions on Biomedical Engineering., 59:1272-80.

[38] Parthasarathy, A.B., Kazmi, S., Dunn, A.K. (2010) Quantitative imaging of ischemic stroke through thinned skull in mice with Multi Exposure Speckle Imaging. Biomed Opt Express. 1: 246-259.

[39] Liu, S., Li, P., Luo, Q. (2008) Fast blood flow visualization of high-resolution laser speckle imaging data using graphics processing unit. Opt Express. 16: 14321-9.

[40] Yang, O., Cuccia, D.J., Choi, B. (2011) Real-time blood flow visualization using the graphics processing unit. J Biomed Opt. 16: 016009.

[41] Richards, L.M., Kazmi,S., Davis,J.L., Olin, K.E., Dunn, A.K. (2013) Low-cost laser speckle contrast imaging of blood flow using a webcam. Biomed Opt Express., 4: 2269-2283.

[42] Jiang, C. Zhang, H., Wang, J., Wang, Y., He, H., Liu, R., Zhou, F., Deng, J., Li, P., Luo, Q. (2011) Dedicated hardware processor and corresponding system-on-chip design for real-time laser speckle imaging. J Biomed Opt. 16: 116008.

[43] Sivakumar, P.S., Kagawa, K., Crouzet, C., Choi, B., Kawahito, S. (2019) Multi-exposure laser speckle contrast imaging using a video-rate multi-tap charge modulation image sensor. Opt Express., 27: 26175.

[44] Kagawa, K. (2021) Functional Imaging with Multi-tap CMOS Pixels. ITE Transactions on Media Technology and Applications., 9: 114-121.

[45] Li, P., Ni, S., Li, Z., Zeng, S., Luo, Q. (2006) Imaging cerebral blood flow through the intact rat skull with temporal laser speckle imaging. Opt Lett., 31: 1824.

[46] Zakharov, P., Vlker, A., Buck, A., Weber, B., Scheffold, F. (2006) Quantitative modeling of laser speckle imaging. Opt lett., 31: 3465-7.

[47] A. Fercher, A.F., Briers, J.D. (1981) Flow visualization by means of single-exposure speckle photography. Opt Commun., 37: 326-330.

[48] Bandyopadhyay, R., Gittings, A.S., Suh, S.S., Dixon, P.K., Durian, D.J. (2005) Speckle-visibility spectroscopy: A tool to study time-varying dynamics. Rev Sci Instrum., 76: 093110.

[49] Ennos, A.E. (1975) Speckle Interferometry.Laser Speckle and Related Phenomena., 9: 203-253.

[50] Kirkpatrick, S.J., Duncan, D.D., Wells-Gray, E.M. (2008) Detrimental effects of speckle-pixel size matching in laser speckle contrast imaging. Opt Lett., 33: 2886-2888.

[51] Vaz, P.G., Member, S., Humeau-Heurtier, A., Figueiras, E., Correia, C., Cardoso, J. (2017) Laser speckle imaging to monitor microvascular

blood flow: a Review. IEEE Reviews in Biomedical Engineering., 9: 106-120.

[52] Basak, K., Manjunatha, M., Dutta, P.K. (2012) Review of laser speckle-based analysis in medical imaging. Med Biol Eng Comput., 50: 547-558.

[53] Thompson, O.B., Andrews, M.K. (2010) Tissue perfusion measurements: multiple-exposure laser speckle analysis generates laser Doppler-like spectra. J Biomed Opt., 15: 027015.

[54] Valdes, C.P., Varma, H.M., Kristoffersen, A.K., Dragojevic, T., Culver, J.P., Durduran, T. (2014) Speckle contrast optical spectroscopy, a non-invasive, diffuse optical method for measuring microvascular blood flow in tissue. Biomed Opt Express., 5: 2769-2784.

[55] Thompson, O.B., Andrews, M.K., Hirst, E. (2011) Correction for spatial averaging in laser speckle contrast analysis. Biomed Opt Express., 2: 1021-1029.

[56] Yuan, S.A., Devor, A., Boas, D.A., Dunn, A.K. (2005) Determination of optimal exposure time for imaging of blood flow changes with laser speckle contrast imaging. Appl Optics., 44: 1823-30.

[57] Parthasarathy, A.B., Tom, W.J., Gopal, A., Zhang, X., Dunn, A.K. (2008) Robust flow measurement with multi-exposure speckle imaging. Opt Express., 16: 1975-89.

[58] Nadort, A., Woolthuis, R.G., Leeuwen, T., Faber, D.J. (2013) Quantitative laser speckle flowmetry of the in vivo microcirculation using sidestream dark field microscopy. Biomed Opt Express., 4: 2347-2361.

[59] Atchia, Y., Levy, H., Dufour, S., Levi, O. (2013) Rapid multiexposure in vivo brain imaging system using vertical cavity surface emitting lasers as a light source. Appl Optics., 52: C64-71.

[60] Kazmi, S.M.S, Balial, S., Dunn,A.K. (2014) Optimization of camera exposure durations for multi-exposure speckle imaging of the microcirculation. Biomed Opt Express., 5: 2157.

[61] Sun, S., Hayes-Gill, B.R., He, D., Zhu, Y., Morgan, S.P. (2015) Multi-exposure laser speckle contrast imaging using a high frame rate CMOS sensor with a field programmable gate array. Opt Lett., 40: 4587-90.

[62] Chammas, M., Pain, F. (2022) Synthetic exposure with a CMOS camera for multiple exposure speckle imaging of blood flow. Sci Rep-UK., 12: 4708.

[63] Briers, J.D., Duncan, D.D., Hirst, E., Kirkpatrick, S.J., Larsson, M., Steenbergen, W., Stromberg, T., Thompson, O.B. (2013) Laser speckle contrast imaging: theoretical and practical limitations. Journal Biomed Opt., 16: 066018.

[64] Forrester, K.R., Stewart, C., Tulip, J., Leonard, C., Bray, R.C. (2002) Comparison of laser speckle and laser Doppler perfusion imaging: measurement in human skin and rabbit articular tissue. Med Biol Eng Comput., 40: 687-97.

[65] Stewart, C.J., Frank, R., Forrester, K.R., Tulip, J., Lindsay, R., Bray, R.C. (2005) A comparison of two laser-based methods for determination of burn scar perfusion: Laser Doppler versus laser speckle imaging. Burns., 31: 744-752.

[66] Millet, C., Roustit, M., Blaise, S., Cracowski, J.L. (2011) Comparison between laser speckle contrast imaging and laser Doppler imaging to assess skin blood flow in humans. Microvasc Res., 82: 147-51.

[67] Garry A.T., Markos, K., Helen C., J David B., Gary J.H. (2011) Comparison of laser speckle contrast imaging with laser Doppler for assessing microvascular function. Microvasc Res., 82: 326-332.

[68] Humeau-Heurtier, A., Mahe, G., Durand, S., Abraham, P. (2013) Skin perfusion evaluation between laser speckle contrast imaging and laser Doppler flowmetry. Opt Commun., 291: 482-487.

[69] Kelsey, S.S., Emma, N.T., Kearsten, B., Rebecca, A.M., James, A.L. (2022) Laser speckle contrast imaging and laser Doppler flowmetry reproducibly assess reflex cutaneous vasoconstriction. Microvasc Res., 142: 104363.

[70] Fredriksson, I., Hultman, M., Strmberg, T., Larsson, M. (2019) Machine learning in multiexposure laser speckle contrast imaging can replace conventional laser Doppler flowmetry. J Biomed Opt., 24: 1-11.

[71] Cheng, W., Lu, J., Zhu, X., Hong,J., Li, P. (2020) Dilated residual learning with skip connections for real-time denoising of laser speckle imaging of blood flow in a log-transformed domain. IEEE Transactions on Medical Imaging., 39: 1582-1593.

[72] Stebakov, I., Kornaeve, E., Stavtsev, D., Potapova, E., Dremin, V. (2021) Laser speckle contrast imaging and machine learning in application to physiological fluids flow rate recognition. Vibroengineering Procedia., 38: 50-55.

[73] Lopez-Tiro, F., Peregrina-Barreto, H., Rangle-Magdaleno, J., Ramirez-San-Juan, J.C. (2021) Localization of blood vessels in in-vitro LSCI images with K-means. In: IEEE International Instrumentation and Measurement Technology Conference. Glasgow, Scotland. 1-5.

[74] Liu, J.X., Gui, Z.G., Zhang, Q., Shang, Y. (2021) Tissue blood flow measurement by diffuse correlation spectroscopy based on Huber regression. Journal of Measurement Science and Instrumentation., 12: 127-132.